Original Article

SMARCA4-deficient non-small cell lung carcinoma: clinicodemographic, computed tomography, and positron emission tomography-computed tomography features

Jong Hee Kim[1#^], Jung Han Woo[1#], Chae Young Lim[1], Taein An[1], Joungho Han[2], Myung Jin Chung[1], Yoon Ki Cha[1]

[1]Department of Radiology and Center for Imaging Science, Samsung Medical Center, Sungkyunkwan University School of Medicine, Seoul, Republic of Korea; [2]Department of Pathology, Samsung Medical Center, Sungkyunkwan University School of Medicine, Seoul, Republic of Korea

Contributions: (I) Conception and design: YK Cha, JH Kim, JH Woo; (II) Administrative support: YK Cha, MJ Chung, J Han; (III) Provision of study materials or patients: YK Cha, JH Kim; (IV) Collection and assembly of data: YK Cha, JH Kim, JH Woo; (V) Data analysis and interpretation: YK Cha, JH Kim, JH Woo; (VI) Manuscript writing: All authors; (VII) Final approval of manuscript: All authors.

[#]These authors contributed equally to this work.

Correspondence to: Yoon Ki Cha, MD, PhD. Department of Radiology and Center for Imaging Science, Samsung Medical Center, Sungkyunkwan University School of Medicine, 81 Irwon-ro, Gangnam-gu, Seoul 06351, Republic of Korea. Email: yoonki.cha@samsung.com.

Background: SMARCA4-deficient non-small cell lung carcinoma (SD-NSCLC) is a relatively rare tumor, which occurs in 5–10% of NSCLC. Based on World Health Organization thoracic tumor classification system, SMARCA4-deficient undifferentiated tumor (SD-UT) is recognized as a separate entity from SD-NSCLC. Differentiation between SD-NSCLC and SD-UT is often difficult due to shared biological continuum, but often required for choosing appropriate treatment regimen. Therefore, the aim of our study was to identify the clinicopathologic, computed tomography (CT), and positron emission tomography (PET)-CT imaging features of SD-NSCLC.

Methods: Nine patients of pathologically confirmed SD-NSCLC were included in our analysis. We reviewed electronic medical records for clinical information, demographic features, CT, and PET-CT imaging features were analyzed.

Results: Smoking history and male predominance are observed in all patients with SD-NSCLC (n=9). On CT, SD-NSCLC appeared as relatively well-defined masses with lobulated contour (n=8) and peripheral location (n=7). Invasion of adjacent pleura or chest wall (n=7) were frequently observed, regardless of small tumor size. Four cases showed lymph node metastases. Among nine patients, three patients showed multiple bone metastases, and one patient showed lung-to-lung metastases.

Conclusions: In patient with SD-NSCLC, there was tendency for male smokers, peripheral location and invasion of adjacent pleural or chest wall invasion regardless of small tumor size, when compared to SD-UT.

Keywords: SMARCA4-deficient non-small cell lung carcinoma (SD-NSCLC); SMARCA4-deficient undifferentiated tumors (SD-UTs); lung cancer; computed tomography (CT); positron emission tomography-computed tomography (PET-CT)

Submitted Oct 19, 2023. Accepted for publication Jan 05, 2024. Published online Mar 08, 2024.
doi: 10.21037/jtd-23-1606
View this article at: https://dx.doi.org/10.21037/jtd-23-1606

^ ORCID: 0000-0002-9090-6484.

Introduction

Over the past decade, there has been a dramatic advancement in the field of non-small cell lung carcinoma (NSCLC) treatment (1). Recent discoveries of mutation in multiple oncogenic driver genes in NSCLC enabled personalized targeted therapy and being readily adapted into clinical practice (2-6). However, despite the recent innovation, many patients still suffer from frequent tumor recurrence and metastasis due to inevitable drug resistance (7). Further study by La Fleur *et al.* have revealed that NSCLC is a complex entity consisting of multiple diseases at a molecular level, which are not only related with oncogenic-based mutations but also tumor suppressor genes mutation due to loss-of-function or deletions (8).

The SMARCA4 gene, which is responsible for the transcription activator BRG1, is one of the most common anomalous ATP-dependent catalytic subunits of SWI/SNF chromatin-remodeling complexes participating in the activation or repression of transcriptional processes in various types of cancer (9). Loss of the BAF (SWI/SNF) complex subunit (also known as BRG1) was first reported in 2000 by Wong *et al.* in various cell lines of prostatic, breast, and pancreatic carcinomas, proving the role of BAF (SWI/SNF) complex as a tumor suppressor gene (10). In thorax, SMARCA4 deficiency appears as two different phenotypes: SMARCA4-deficient undifferentiated tumor (SD-UT; formerly known as SMARCA4-deficient sarcoma) and SMARCA4-deficient non-small cell lung carcinoma (SD-NSCLC). Previous study of Reisman *et al.* have shown that SMARCA4 deficiency can be occasionally seen in conventional NSCLC with poorer prognosis (11). In 2015, Le Loarer *et al.* reported a case series of SD-UT in 19 patients with following features: young male smokers, a rapidly enlarging thoracic mass with rhabdoid morphological features, undifferentiated immunophenotype, and a very aggressive clinical course (12).

Currently, SD-NSCLC is recognized as relatively rare tumor, which occurs in 5–10% of NSCLC (13). According to the 8th edition of World Health Organization (WHO) thoracic tumor classification system, only SD-UT is recognized as a separate disease entity, distinguished from SD-NSCLC (14). However, differentiation between SD-NSCLC and SD-UT may be difficult and sometimes impossible due to the shared biological continuum between both entities (15). In fact, these tumors are closely linked at a molecular level as they share the same genomic alterations, which is typical of smoking related NSCLC (KRAS, KEAP1, STK11) and a high tumor mutational load (12,16). For treatment of SD-NSCLC, radical surgical excision which resulted in complete remission in resectable cases has been reported (17); however, it is often presented at an advanced stage and generally insensitive to palliative treatment such as chemotherapy and radiotherapy (18). Recently, immune checkpoint blockade (ICB) has shown a promising but inconsistent response in SMARCA4-mutant NSCLC, from favorable to poor or even hyper-progression (19,20). Although yet to be evaluated, the presence of SMARCA4 mutations opens a wide variety of therapeutic possibilities using targeted therapy (21).

To the best of our knowledge, there have been only few studies regarding SD-NSCLC, especially with emphasis on the imaging features of computed tomography (CT), and positron emission tomography (PET)-CT (18,22). Therefore, the aim of our study was to retrospectively assess the clinical, demographic, and imaging features of SD-NSCLC, and compare with previous reported features of SD-UT to observe possible differentiating characteristics. We present this article in accordance with the STROBE reporting checklist (available at https://jtd.amegroups.com/article/view/10.21037/jtd-23-1606/rc).

Highlight box

Key findings

- Possibility of SMARCA4-deficient non-small cell lung carcinoma (SD-NSCLC) should be considered when confronted with peripherally located lung tumors showing invasion of adjacent pleura or chest wall regardless of small tumor size, especially among male smokers.

What is known and what is new?

- Differentiation between SD-NSCLC and SMARCA4-deficient undifferentiated tumor is often difficult due to shared biological continuum, but often required for choosing appropriate treatment regimen.
- On computed tomography, SD-NSCLC appeared as relatively well-defined masses with lobulated contour (eight out of nine cases) and peripheral location (seven out of nine cases). Invasion of adjacent pleura or chest wall (seven out of nine cases) were frequently observed, regardless of small tumor size.

What is the implication, and what should change now?

- In male smokers presenting with peripherally located tumors and showing invasion of adjacent pleura or chest wall regardless of small tumor size, radiologists should be concerned about the possibility of SD-NSCLC.

Methods

Patient selection

The study was conducted in accordance with the Declaration of Helsinki (as revised in 2013). The institutional review board of Samsung Medical Center approved this retrospective study (IRB file No.: 2023-02-010), and the requirement for patient consent to use clinical data was waived due to retrospective study design. We searched electronic medical records between January 2018 to November 2022, among patients who underwent transbronchial lung or lymph node biopsy, percutaneous core needle lung biopsy, and curative lung resection surgery at Samsung Medical Center, a tertiary referral hospital located in Seoul, Republic of Korea. By using the term "SMARCA4 deficient non-small cell lung cancer", we found nine patients with pathological confirmation of SD-NSCLC.

Clinical and pathologic assessment

Two of the authors (J.H.K., Y.K.C.) reviewed electronic medical records for clinicopathologic data of the patients, as follows: age, sex, smoking history, and pack-years if available. In all nine patients, the histopathologic reports were recorded. Five patients underwent curative resection, and subsequently staged based on the 8th edition of the American Joint Committee on Cancer (AJCC) TNM classification. Pathologic specimens were examined by pathologists who reported the pathologic findings using the latest edition of the WHO classification thoracic tumor classification system. In four patients without surgical resection, diagnosis of SD-NSCLC was confirmed through either percutaneous lung (n=1) or lymph node (n=3) biopsy.

Image acquisition

CT studies from various helical CT scanners (from 16- to 64-MDCT scanners) from several vendors were performed. The scanning parameters were 120 kVp and 100 to 150 mAs under automatic exposure control; beam width, 10 to 20 mm; and rotation time, 0.3 to 0.4 seconds. CT image data were reconstructed using standard soft-tissue algorithms, with a section thickness of 2.5 to 3.0 mm for axial images. Both contrast and noncontrast CT scans were obtained. Intravenous (IV) contrast medium injection was given in all patients: 1.5 mL/kg of body weight of iobitridol (300 mg I/mL; Xenetics, Guerbet, Aulnay-sous-Bois, France) was injected at an infusion rate of 3 mL/s using a power injector (MCT Plus, Medrad, Pittsburgh, USA). Both mediastinal (width, 400 HU; level, 20 HU) and lung (width, 1,500 HU; level, −700 HU) window settings were adapted during image review.

All nine patients included in our analysis performed both CT and PET-CT studies in our institution. Before PET-CT examinations, all patients fasted for at least 6 hours. Blood glucose level was measured before injection of ^{18}F-fluorodeoxyglucose (FDG), targeting <150 mg/dL for the examination. Whole-body PET and noncontrast CT images were performed using two PET-CT scanners (Discovery LS and Discovery STe, GE Healthcare, Chicago, USA) 60 minutes after FDG injection (5.5 MBq/kg). A whole-body CT with Discovery LS scanner adapted continuous helical technique with 8-MDCT (140 keV; 40–120 mAs; section width, 5 mm). PET was acquired from the head to middle thigh for 4 minutes per frame in the 2D mode after CT scan. Attenuation-corrected PET images (4.3×4.3×3.9 mm) were reconstructed from the CT data using an ordered subset expectation maximum (OSEM) algorithm (28 subsets, 2 iterations). A whole-body CT with Discovery STe scanner adapted a continuous helical technique with 16-MDCT (140 keV; 30–170 mAs; section width, 3.75 mm). PET scans were obtained from the head to middle thigh for 2.5 minutes per frame in the 3D mode after CT scan. Attenuation-corrected PET images (3.9×3.9×3.3 mm) were reconstructed from the CT data using a 3D OSEM algorithm (20 subsets, 2 iterations). The standardized uptake value (SUV) was calculated based on the injected dose of FDG and body weight of the patient.

Image interpretation

CT studies were reviewed by three radiologists with thoracic CT interpretation experience of 5, 8 and 16 years, and all decisions were made by consensus. Multiple CT imaging features were assessed: tumor size (maximum, in mm), attenuation value (in HUs), net enhancement (attenuation difference between enhanced and unenhanced images), tumor margin (well or poorly defined), contour (round, lobulated, or spiculated), presence of necrotic component, calcification, and pleural tagging within the primary tumor. Tumor size was determined as the longest diameter among three planes (axial, coronal, and sagittal). When measuring tumor attenuation, the region of interest (ROI) covering more than half of the tumor diameter was adopted on both enhanced and unenhanced images and values were

Table 1 Demographic features and clinical findings of nine patients with SMARCA4-deficient non-small cell lung cancer

Variables	All patients (n=9)
Age (years)	64 (46–74)
Male	9 (100.0)
Smoking history	
Current smoker	5 (55.6)
Ex-smoker	4 (44.4)
Never smoker	0
Average pack-years	51.9 (17–140)
CT visual classification of emphysema	
Present	5 (55.6)
Mild	5
Moderate	0
Confluent	0
Advanced destructive	0
Absence	4 (44.4)
Symptoms	
Yes	1 (11.1)
No	8 (88.9)
Treatment	
Surgical resection	5 (55.6)
Palliative	4 (44.4)

The data are presented as median value (range) or number (%). CT, computed tomography.

subtracted to calculate the net enhancement. Tumor margin was characterized as either well- or poorly-defined. A well-defined margin was defined as a distinct interface between a lesion and the surrounding parenchyma at more than 50% of the imaged circumference and otherwise considered as poorly defined. Contour was described as round, lobulated, or spiculated. A spiculated margin was defined as a thickening and distorted line radiating from the nodular surface. The tumor distribution was determined by dividing the lung into inner and outer regions at the midline on CT images. Tumors with their center located medial to the midline were considered central, and those located lateral to the midline were considered peripheral (23). Additional image findings such as enlarged lymph nodes in the hilum (>10 mm in short axis) and mediastinum (>10 mm in short axis), presence of pleural thickening or nodularity, and pleural effusion were also evaluated.

Due to high prevalence of smokers in SMARCA4-deficient tumor, we also evaluated the presence of emphysema and subsequently graded based on Fleischner Society CT-based visual classification (mild, moderate, confluent, and advanced destructive emphysema) (9,24). In PET-CT, the FDG uptake of the tumor was compared with that of the mediastinal blood pool. Positive uptake was defined as higher FDG uptake of the tumor than of the mediastinal blood pool. Then SUV was measured, and the maximum SUV (SUV_{max}) was determined. Furthermore, FDG uptake pattern were also evaluated and categorized into three patterns: diffuse, curvilinear, or crisscross patterns.

Statistical analysis

The presentation of continuous variables included the mean and range, while categorical variables were expressed as counts and percentages (%). All statistical analyses were performed using SPSS (version 25.0).

Results

Demographic and clinical findings

Demographic and clinical features of nine cases of SD-NSCLC are summarized in *Table 1*. All patients were male and the median age at the time of diagnosis was 64 years (range, 46–74 years). Only one (11.1%) patient had symptoms of hoarseness, cough, and sputum at initial presentation. Eight (88.9%) patients were asymptomatic and incidentally diagnosed through routine heath check-up. All nine patients were either current or ex-smokers (five current smokers, four ex-smokers; average pack-years, 51.9).

Imaging findings

Characteristic imaging features with detailed description of all cases of SD-NSCLC are summarized in *Tables 2,3*. In CT, tumors were in form of either solitary nodules (n=4, 44.4%) or masses (n=5, 55.6%). Median tumor size was 42 mm (range, 8–62 mm) and all tumors showed well-defined margins (n=9). Most tumors appeared as lobulated contour (n=8, 88.9%), and only one case showed spiculation. After IV injection of contrast medium, measured net enhancement values ranged from 8 to 43 HU (median, 24 HU). There was no evidence of

Table 2 Image findings of SMARCA4-deficient non-small cell lung cancer

CT imaging finding	All patients (n=9)
Tumor location	
RUL	3 (33.3)
RLL	2 (22.2)
LUL	4 (44.4)
Distribution	
Central	2 (22.2)
Peripheral	7 (77.8)
Margin	
Well marginated	9 (100.0)
Ill-defined	0
Shaped	
Round	0
Lobulated	8 (88.9)
Spiculated	1 (11.1)
Mean precontrast/postcontrast (HU)	25.4 (11–46)/52.2 (24–79)
Mean Δ HU	24±12.3
Calcification	
No	9 (100.0)
Necrosis	
No	9 (100.0)
Pleural tagging	
Yes	1 (11.1)
No	8 (88.9)
Pleural effusion	
Yes	2 (22.2)
No	7 (77.8)
Pleura and chest wall invasion	
Yes	7 (77.8)
No	2 (22.2)
Lymph node enlargement	
Yes	5 (55.6)
No	4 (44.4)
Intrathoracic metastasis	
Yes	5 (55.6)
No	4 (44.4)
Extrathoracic metastasis	
Yes	3 (33.3)
No	6 (66.7)
^{18}F-FDG PET-CT	
SUV_{max}	13.5 (9.6–16.5)

The data are presented as median value (range), number (%), or mean ± standard deviation. CT, computed tomography; RUL, right upper lobe; RLL, right lower lobe; LUL, left upper lobe; HU, Hounsfield unit; ^{18}F-FDG, ^{18}F-fluorodeoxyglucose; PET-CT, positron emission tomography-computed tomography; SUV_{max}, maximum standardized uptake value.

necrotic change or calcification within the tumors in all nine cases. In seven (77.8%) patients, the tumors were located at the peripheral portion of the lung, and only two (22.2%) cases were located at the central portion. In seven (77.8%) cases, the tumors showed direct pleural and chest wall invasion, regardless of small tumor size (*Figure 1*). Five (55.6%) of nine patients showed enlarged lymph nodes in hilar, mediastinal, and supraclavicular areas, and two (22.2%) patients showed necrotic changes within the enlarged lymph nodes (*Figure 2*). All nine patients had smoking history, and five (55.6%) patients showed mild degree of centrilobular emphysema in CT, graded based on the Fleischner Society CT-based visual classification. For metastasis, four (44.4%) patients showed intra- or extrathoracic metastasis at the time of diagnosis. Metastases involved bone in three (33.3%) patients (all with multiple areas), and lung in one (11.1%) patient.

FDG PET-CT and pathologic findings

FDG PET-CT was performed in all nine patients included in our analysis. FDG accumulation within the tumor was relatively intense, and the median value of measured SUV_{max} was 13.5 (range, 9.5–16.5). In all cases, there were diffuse uptake patterns, and no curvilinear nor crisscross patterns were observed.

All nine cases showed presence of differentiated histology in pathologic specimens (either glandular or squamous). Presence of differentiated histology in SD-NSCLC is known to be a distinct feature from SD-UT, as SD-UT are generally associated with undifferentiated or rhabdoid morphology (25). Moreover, all nine cases showed TTF1

Table 3 Clinical and imaging feature of thoracic SMARCA4-deficient non-small cell lung cancer

Age (years)/ sex	Pack-years	Lobe	Location	CT imaging features						PET-CT features		Treatment		
				Size (mm)	Mean HU	Shape	Pleural/chest wall invasion	Lymph node metastasis	Distant metastasis	SUV_{max}	FDG uptake pattern	Treatment	TNM	F/U
67/M	45	RLL	Central	42	18	Lobulated	None	Interlobar	Bone	N/A	Diffuse	CTx	N/A	Under treatment
59/M	17	LUL	Peripheral	61	12	Lobulated	Pleural	None	None	14.1	Diffuse	Lobectomy + adj. CTx	T4N0	NED
67/M	40	LUL	Peripheral	23	35	Lobulated	Pleural	None	None	12.7	Diffuse	Lobectomy + adj. CCRTx	T3N0	NED
62/M	40	LUL	Peripheral	15	40	Lobulated	Pleural	Ipsilateral hilar, para-aortic	Bone	16.5	Diffuse	CTx	N/A	Expired
67/M	140	RUL	Peripheral	8	43	Lobulated	None	None	None	12.9	Diffuse	Lobectomy	T1bN0	NED
46/M	30	RUL	Peripheral	62	8	Lobulated	Pleural	None	None	N/A	Diffuse	Lobectomy + adj. CTx	T3N0	Under treatment
74/M	80	LUL	Peripheral	61	40	Spiculated	Pleural	Both supraclavicular, mediastina, hilar, ipsilateral interlobar	Bone	9.6	Diffuse	CTx	N/A	Under treatment
63/M	30	RLL	Peripheral	27	21	Lobulated	Pleural	Ipsilateral hilar, interlobar, peribronchial, subcarinal	Lung-to-lung	14.9	Diffuse	CTx	N/A	Under treatment
69/M	45	RUL	Central	42	24	Lobulated	Pleural	None	None	N/A	Diffuse	Lobectomy + adj. CTx	T2bN0	Under treatment

CT, computed tomography; HU, Hounsfield unit; PET-CT, positron emission tomography-computed tomography; SUV_{max}, maximum standardized uptake value; FDG, fluorodeoxyglucose; F/U, follow-up; RLL, right lower lobe; CTx, chemotherapy; N/A, not available; LUL, left upper lobe; adj. CTx, adjuvant chemotherapy; NED, no evidence of disease; adj. CCRTx, adjuvant concurrent chemoradiation; RUL, right upper lobe.

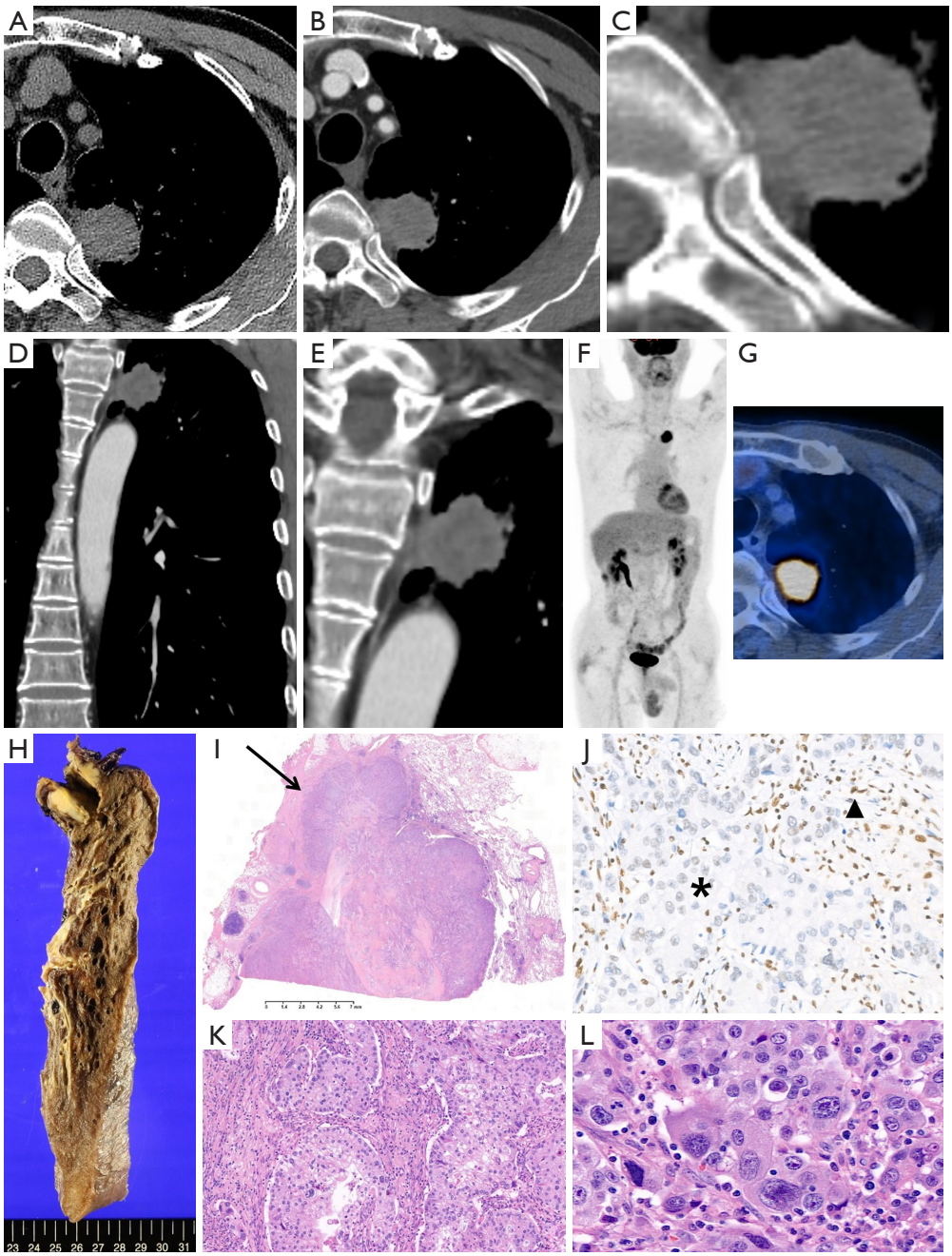

Figure 1 A representative case of SMARCA4-deficient non-small cell lung cancer. A 67-year-old man presented with left upper lobe nodule, incidentally detected during health check-up. Unenhanced and enhanced CT scan (A,B) shows a 26 mm sized relatively well-defined subpleural nodule in left upper lobe, and it shows heterogeneous enhancement (ΔHU =35). On axial and coronal enhanced CT scan (C-E) left upper lobe nodule shows invasion to adjacent chest wall. On MIP (F) and fusion image of PET-CT (G), the nodule shows diffuse and intense ^{18}F-FDG uptake, showing SUV_{max} of 12.7. (H) The photograph of gross specimen shows 28×28×20 mm sized mass, and (I) photomicrograph obtained at low magnification shows invasion of the tumor (arrow; hematoxylin and eosin stain) to adjacent chest wall. Photomicrograph (hematoxylin and eosin stain) shows two different cores within the tumor; (K) areas with poorly differentiated adenocarcinoma (hematoxylin and eosin stain, ×100), (L) large pleomorphic tumor cells (hematoxylin and eosin stain, ×400). On BRG1 (SMARCA4) immunostaining (J), it shows a loss of SMARCA4 nuclear expression in tumor cells (*) in contrast with normally stained inflammatory cells (▲) (BRG1 immunohistochemical stain, ×400). CT, computed tomography; MIP, maximum-intensity-projection; PET, positron emission tomography; FDG, fluorodeoxyglucose; SUV_{max}, maximum standardized uptake value.

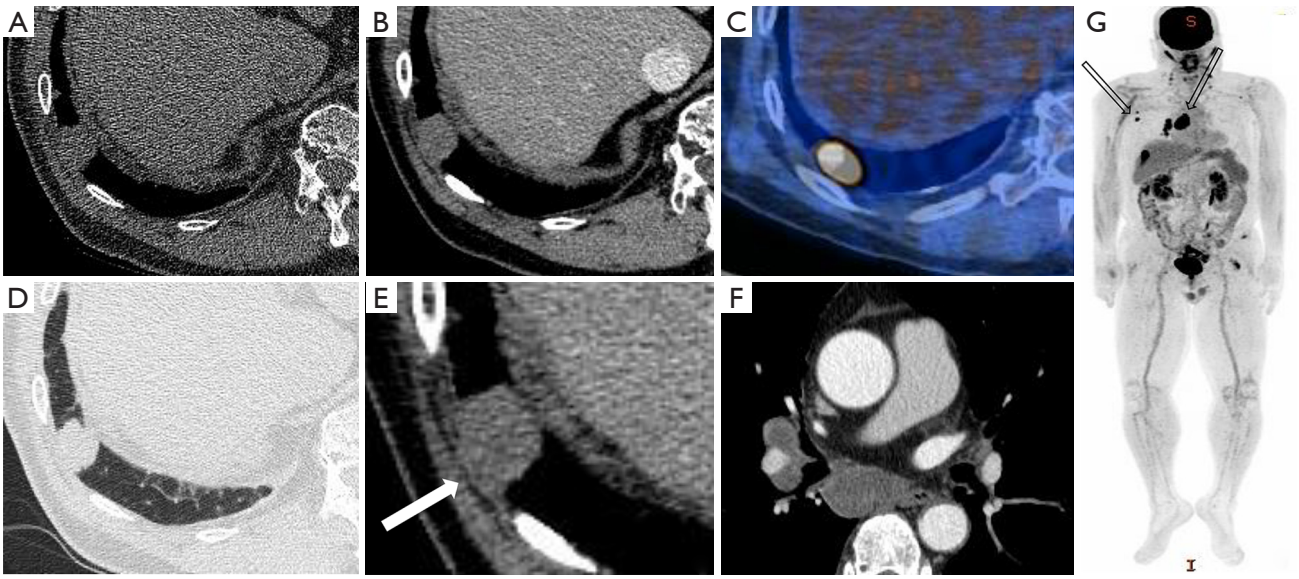

Figure 2 A 63-year-old man with SMARCA4-deficient non-small cell lung cancer. Unenhanced (A,D) and enhanced (B,E) CT scans show enhancing nodule with lobulated contour in right lower lobe periphery, and the nodule shows chest wall invasion (arrow). On enhanced CT (F), it shows multiple enlarged lymph nodes with necrotic changes in subcarinal and right interlobar areas. On MIP (G) and fusion image of PET-CT (C), the nodule shows diffuse intense FDG uptake (SUV_{max} =14.9). On MIP (G) right axillary, right hilar and right mediastinal also show FDG uptake (open arrows), suggesting metastasis. CT, computed tomography; MIP, maximum-intensity-projection; PET, positron emission tomography; FDG, fluorodeoxyglucose; SUV_{max}, maximum standardized uptake value.

negativity, which is known to be found in 80% of SWI/SNF-deficient lung adenocarcinoma, which led to further evaluation of SMARCA4 (BRG1) and SMARCA2 (BRM).

Treatment and prognosis

Five (55.6%) patients received surgical resection with mediastinal lymph node dissection, and the resection was complete with negative resection margin in all cases. Mediastinal nodal metastases were not observed. In two (22.2%) patients, tumor invasion of parietal pleura of the chest wall was observed, and other two patients showed superficial invasion of pleural connective tissue, not beyond the elastic layer of the visceral pleura. After surgical resection was performed, three (60%) of five patients had performed adjuvant chemotherapy. All five patients who had undergone the curative resection have survived and there was no recurrence on follow-up imaging studies.

Four (44.4%) patients who had intra- or extrathoracic metastatic disease at the time of diagnosis, palliative chemotherapy was performed instead of surgical resection. Two of four patients with chemotherapy showed poor clinical outcomes. One patient showed very poor clinical outcome (expired within 6 months of chemotherapy), and another patient showed rapid disease progression in the form of new metastasis involving bone, within 4 months after treatment. In other two patients with chemotherapy, the primary tumor and metastatic lesions showed overall decrease in size and extent during follow-up. In overall, eight of nine patients survived after median follow-up periods of 5.2 months (range, 2–10 months).

Discussion

Due to the rarity of SD-NSCLC, only a very limited number of research regarding CT and PET-CT imaging and clinicopathologic features of SD-NSCLC have been reported to date (26,27). To the best of our knowledge, our study is the largest to focus on the clinical, imaging, and pathologic findings of the SD-NSCLC. Our results showed that SD-NSCLC has a strong tendency to show a peripheral distribution, lobulated contour, high proportion of pleural invasion regardless of small size, and clinical predilection of male patients with smoking history. Currently, distinction between SD-NSCLC and SD-UT is required not only for the accurate diagnosis according to WHO classification of

lung tumors, but also for the appropriate targeted therapies which is often crucial for patient survival (14,18). However, in small biopsies with poor morphology, unusual immune profiles and with sarcomatoid areas, differentiation between SMARCA4-deficient NSCLC and SMARCA4-UT is difficult and sometimes impossible (18). Genomic profiling is unlikely to add diagnostic value, since SMARCA4-deficient NSCLC usually harbor truncating SMARCA4 mutations (>90% of NSCLC with BRG1 loss harbor truncating SMARCA4 mutations) and shows overlapping molecular profiles with SMARCA4-UT (TP53, KRAS, STK11, and KEAP1 mutations) and high tumor mutation burden (18). It seems reasonable to assume the biological continuum between these two tumors, as they share genomic alterations typical of smoking related NSCLC (KRAS, KEAP1, STK11) (12,16).

Demographic features of SD-NSCLC in our study showed similarities in terms of male predominance and smoking history (five current smokers, four ex-smokers; average pack-years, 51.9) with reported features of SD-UT. This result also correlates with the previous studies of SD-NSCLC (13,28). However, in our study, most patients were asymptomatic, and the tumors were incidentally diagnosed during the routine health check-up. In five patients who underwent curative resection, three cases were detected at a relatively earlier stage. In contrast, patients with SD-UT are frequently symptomatic with most frequent symptoms being dyspnea. Also, indirect symptoms of regional invasion were frequently observed, such as superior vena cava syndrome, Pancoast syndrome, and hemoptysis (29).

According to our study, the majority of SD-NSCLC was manifested as relatively well-defined nodules or masses, showing lobulated contour and variable degree of enhancement. This result shows difference from previous study by Lou *et al.* (26). Lou *et al.* have reported 23 cases of SD-NSCLC in 2022, which mostly manifested as infiltrative masses and heterogenous densities with unclear margins (26). These image findings were in contrary to our study, and we believe such differences might be due to the fact that large proportion of our cohort were detected earlier phase during routine health check-up. Moreover, our study showed clearly distinguishable imaging features from SD-UT, which showed ill-defined margin in all patients (21 cases) (29). SD-NSCLC in our cohort did not show any calcification nor necrotic components, which was coherent with reported imaging features of SD-UT (29). Most of the SD-NSCLC were in the peripheral portion of the lung (n=7, 77.8%), and showed adjacent pleura and chest wall invasion regardless of small tumor size. It has been known that SD-NSCLC has highly aggressive behavior with vascular invasion and pleural metastasis (30), and high prevalence of pleural and chest wall metastasis might be due to SMARCA4 relation with trans-membrane glycoprotein CD44, which is closely related to metastasis (9,31). Furthermore, the incidence of pleural invasion was higher in our study when compared with the previous study of Heidinger *et al.* in terms of pleural invasion of pulmonary adenocarcinomas, according to CT features of primary tumor (32). In our study, the incidence of pleural invasion was observed to be 77.8%, whereas Heidinger *et al.* reported 24.6% in solid tumors and 4.7% in subsolid tumors (32). However, since our study included only small number of patients, further research with larger cohort would be necessary for more accurate comparison. Regarding metastatic potential of SD-UT, Crombé *et al.* have mentioned a striking tendency of SD-UT to cross compartments and to spread from mediastinum to pleura, neck, or lung apex in an infiltrative and compressive fashion (29). We assumed the same principle can be adopted to explain our cases of SD-NSCLC with relatively aggressive pleural and chest wall invasion regardless of tumor size.

In terms of nodal metastasis, four (44%) cases showed metastatic lymph nodes with two cases of necrosis within the lymph nodes in CT. In five cases with curative surgical resection, pathologic lymph node metastases were not observed in all cases. This result is similar to the previous pathologic study of SD-NSCLC, which reported lymph node metastases in 47% of all cases (13). Furthermore, based on previous study regarding tumor genomic features associated with pathologic lymph node metastasis in clinical stage I and II, an alteration in SMARCA4 gene was significantly associated with higher lymph node metastasis (33). Lymph node involvement in SD-UT is also known to show heterogeneous (necrotic) attenuation with ill-defined perinodal soft tissue infiltration (15,18). In previous study of SD-UT, almost all cases showed lymph node metastases with necrotic change (29). We believe that the correlation between SMARCA4 deficiency and pathologic lymph node metastasis with tendency for necrosis was also demonstrated through our analysis.

Proportion of distant metastases at the time of diagnosis in SD-NSCLC was similar to that of previous study of SD-UT (29). Our study revealed that four patients had intra- or extrathoracic metastasis at the time of diagnosis. Metastases involved the bone in three patients (all with multiple areas), and lung in one patient. We carefully

hypothesized that SD-NSCLC and SD-UT may share similarity in terms of distant metastases, probably based on the molecular similarity in the molecular level. Also, in PET-CT, all tumors in lung parenchyma showed diffuse and intense FDG uptake with SUV_{max} value ranging from 9.5–16.5 in the lung parenchyma. This was coherent with previous study regarding SMARCA4-UT, which reported strong FDG avidity with mean SUV_{max} of 16.6 (range, 9.1–33.8) (29). Herein, we can assume that PET-CT features including SUV_{max} value and FDG uptake pattern of SD-NSCLC is in fact similar to that of SD-UT.

In terms of pathologic diagnosis of SD-UT and SD-NSCLC, SD-NSCLC is usually distinguished from SD-UT based on the morphology by well-differentiation in form of clear-cut adenocarcinoma or very rarely, squamous cell carcinoma (18). Unlike SD-UT, differentiated (glandular or squamous) histology is more frequent in SD-NSCLC (34). Also, SMARCA4 and SMARCA2 should be included in the workup of TTF1-negative adenocarcinoma of presumable pulmonary origin, as 80% of SMARCA4/SMARCA2-deficient lung adenocarcinomas are TTF1 negative (34). In contrary, SD-UT is known to consist of diffuse sheets of variably discohesive, large, round to epithelioid cells with vesicular chromatin and prominent nucleoli (14). Unequivocal epithelial architecture (e.g., glandular or squamous differentiation) should be absent, except rare, combined cases in which conventional NSCLC is juxtaposed (14).

SD-NSCLC is known to be associated with overall poorer outcome independent of clinical stages (9,13). Inconsistent responses to ICB have been observed in SD-NSCLC with variable responses, from favorable, poor to even hyper-progression (18). This might be partly explained by the high co-occurrence of STK11 and KEAP1 mutations in SD-NSCLC that are known to blunt responses to immune checkpoint inhibitors (ICIs) (14). Regarding the relationship between SD-NSCLC and SD-UT, recent study by Lin *et al.* demonstrated survival benefit of ICI comparing to traditional chemotherapy in SD-UT, and the prognostic disparity between SD-NSCLC and SD-UT under different treatment settings (35). ICI-based treatment significantly improved progression-free survival (PFS) than chemotherapy in the first-line treatment of SD-UT (35). Moreover, patients of SD-UT and SD-NSCLC receiving ICI-based regimen as first-line treatment had significantly longer median overall survival than those having ICI-based regimen in latter line or no ICI treatment throughout clinical courses (35). These results indicated the promising efficacy of ICI in metastatic SD-UT, and its optimal effect may be achieved when used early in clinical courses (35). Regarding the prognostic disparity, no significant survival differences were observed in PFS between SD-UT and SD-NSCLC of under same treatment settings (35). However, some studies showed limited efficacy of ICI in SD-UT. Gantzer *et al.* reported that SD-UT mostly had an immune-desert tumor microenvironment (36). Only one out of four patients in Gantzer's cohort turned out to have immune-rich tumor microenvironment responded to ICI (36). However, despite multimodal treatment therapy including chemotherapy and surgery, the clinical outcomes of most patients with SD-NSCLC and SD-UT have been discouraging to date (18,35). Due to the small sized cohort, the prognosis of each patient with SD-NSCLC could not be exactly compared with SD-UT. In our case series, eight (88.9%) of nine patients have survived. Although long-term clinical outcomes are not available, tumors with relatively low-grade TNM stage tend to show excellent short-term results. In five cases who have undergone curative resection with or without adjuvant chemotherapy, there was no evidence of recurrence during the follow-up periods. In patients with palliative chemotherapy without surgery, most patients showed an overall decrease in the extent of total tumor burden. However, like SD-UT behavior, early relapse or progression more frequently occurred (29). In the previous study of SD-UT, all patients died of their disease due to local complications, with a median survival of 5 months after initial diagnosis.

Our study has several limitations. First, our analysis was conducted based on a retrospective design with small number of patients due to rarity of disease entity. However, to our knowledge, this study is the largest cohort to provide detailed analyses of clinicodemographic, CT and PET-CT imaging features of SD-NSCLC. Second, our follow-up period was relatively short with a median value of 6 months. Larger cohort with long-term follow-up study is mandatory to better understand the tumor behavior and prognosis. Furthermore, studies focusing on the comparison of image finding with other histopathologic types and mutations of primary lung cancer are required to further validate our results.

Conclusions

In conclusion, SD-NSCLC is a rare type of primary lung cancer which shows similar demographic and clinical features with SD-UT. In male smokers presenting with peripherally located tumors and showing invasion of adjacent pleura or chest wall regardless of small tumor size,

radiologists should be concerned about the possibility of SD-NSCLC.

Acknowledgments

Funding: None.

Footnote

Reporting Checklist: The authors have completed the STROBE reporting checklist. Available at https://jtd.amegroups.com/article/view/10.21037/jtd-23-1606/rc

Data Sharing Statement: Available at https://jtd.amegroups.com/article/view/10.21037/jtd-23-1606/dss

Peer Review File: Available at https://jtd.amegroups.com/article/view/10.21037/jtd-23-1606/prf

Conflicts of Interest: All authors have completed the ICMJE uniform disclosure form (available at https://jtd.amegroups.com/article/view/10.21037/jtd-23-1606/coif). The authors have no conflicts of interest to declare.

Ethical Statement: The authors are accountable for all aspects of the work in ensuring that questions related to the accuracy or integrity of any part of the work are appropriately investigated and resolved. The study was conducted in accordance with the Declaration of Helsinki (as revised in 2013). The institutional review board of Samsung Medical Center approved this retrospective study (IRB file No.: 2023-02-010), and the requirement for patient consent to use clinical data was waived due to retrospective study design.

References

1. Reck M, Remon J, Hellmann MD. First-Line Immunotherapy for Non-Small-Cell Lung Cancer. J Clin Oncol 2022;40:586-97.
2. Tan AC, Tan DSW. Targeted Therapies for Lung Cancer Patients With Oncogenic Driver Molecular Alterations. J Clin Oncol 2022;40:611-25.
3. Borghaei H, Gettinger S, Vokes EE, et al. Five-Year Outcomes From the Randomized, Phase III Trials CheckMate 017 and 057: Nivolumab Versus Docetaxel in Previously Treated Non-Small-Cell Lung Cancer. J Clin Oncol 2021;39:723-33.
4. Herbst RS, Garon EB, Kim DW, et al. Five Year Survival Update From KEYNOTE-010: Pembrolizumab Versus Docetaxel for Previously Treated, Programmed Death-Ligand 1-Positive Advanced NSCLC. J Thorac Oncol 2021;16:1718-32.
5. Mazieres J, Rittmeyer A, Gadgeel S, et al. Atezolizumab Versus Docetaxel in Pretreated Patients With NSCLC: Final Results From the Randomized Phase 2 POPLAR and Phase 3 OAK Clinical Trials. J Thorac Oncol 2021;16:140-50.
6. Peters S, Reck M, Smit EF, et al. How to make the best use of immunotherapy as first-line treatment of advanced/metastatic non-small-cell lung cancer. Ann Oncol 2019;30:884-96.
7. Passaro A, Brahmer J, Antonia S, et al. Managing Resistance to Immune Checkpoint Inhibitors in Lung Cancer: Treatment and Novel Strategies. J Clin Oncol 2022;40:598-610.
8. La Fleur L, Falk-Sörqvist E, Smeds P, et al. Mutation patterns in a population-based non-small cell lung cancer cohort and prognostic impact of concomitant mutations in KRAS and TP53 or STK11. Lung Cancer 2019;130:50-8.
9. Tian Y, Xu L, Li X, et al. SMARCA4: Current status and future perspectives in non-small-cell lung cancer. Cancer Lett 2023;554:216022.
10. Wong AK, Shanahan F, Chen Y, et al. BRG1, a component of the SWI-SNF complex, is mutated in multiple human tumor cell lines. Cancer Res 2000;60:6171-7.
11. Reisman DN, Sciarrotta J, Wang W, et al. Loss of BRG1/BRM in human lung cancer cell lines and primary lung cancers: correlation with poor prognosis. Cancer Res 2003;63:560-6.
12. Le Loarer F, Watson S, Pierron G, et al. SMARCA4 inactivation defines a group of undifferentiated thoracic malignancies transcriptionally related to BAF-deficient sarcomas. Nat Genet 2015;47:1200-5.
13. Velut Y, Decroix E, Blons H, et al. SMARCA4-deficient lung carcinoma is an aggressive tumor highly infiltrated by FOXP3+ cells and neutrophils. Lung Cancer 2022;169:13-21.

14. Nicholson AG, Tsao MS, Beasley MB, et al. The 2021 WHO Classification of Lung Tumors: Impact of Advances Since 2015. J Thorac Oncol 2022;17:362-87.
15. Rekhtman N, Montecalvo J, Chang JC, et al. SMARCA4-Deficient Thoracic Sarcomatoid Tumors Represent Primarily Smoking-Related Undifferentiated Carcinomas Rather Than Primary Thoracic Sarcomas. J Thorac Oncol 2020;15:231-47.
16. Yoshida A, Kobayashi E, Kubo T, et al. Clinicopathological and molecular characterization of SMARCA4-deficient thoracic sarcomas with comparison to potentially related entities. Mod Pathol 2017;30:797-809.
17. Zheng MJ, Zheng Q, Wang Y, et al. SMARCA4-deficient primary thoracic sarcoma:a clinicopathological analysis of five cases. Zhonghua Bing Li Xue Za Zhi 2019;48:537-42.
18. Nambirajan A, Jain D. Recent updates in thoracic SMARCA4-deficient undifferentiated tumor. Semin Diagn Pathol 2021;38:83-9.
19. Schoenfeld AJ, Bandlamudi C, Lavery JA, et al. The Genomic Landscape of SMARCA4 Alterations and Associations with Outcomes in Patients with Lung Cancer. Clin Cancer Res 2020;26:5701-8.
20. Dagogo-Jack I, Schrock AB, Kem M, et al. Clinicopathologic Characteristics of BRG1-Deficient NSCLC. J Thorac Oncol 2020;15:766-76.
21. Italiano A, Soria JC, Toulmonde M, et al. Tazemetostat, an EZH2 inhibitor, in relapsed or refractory B-cell non-Hodgkin lymphoma and advanced solid tumours: a first-in-human, open-label, phase 1 study. Lancet Oncol 2018;19:649-59.
22. Mehta A, Diwan H, Bansal D, et al. TTF1-positive SMARCA4/BRG1 deficient lung adenocarcinoma. J Pathol Transl Med 2022;56:53-6.
23. Kim CH, Cha YK, Han J, et al. CT findings of basaloid squamous cell carcinoma of the lung in 12 patients: A distinct category of squamous cell carcinoma in 2015 WHO classification of lung tumors. Medicine (Baltimore) 2022;101:e29197.
24. Shang Y, Li X, Liu W, et al. Comprehensive genomic profile of Chinese lung cancer patients and mutation characteristics of individuals resistant to icotinib/gefitinib. Sci Rep 2020;10:20243.
25. Sauter JL, Graham RP, Larsen BT, et al. SMARCA4-deficient thoracic sarcoma: a distinctive clinicopathological entity with undifferentiated rhabdoid morphology and aggressive behavior. Mod Pathol 2017;30:1422-32.
26. Lou C, Zhao H, Lu H, et al. Clinical, Radiological and Pathological Features of SMARCA4 / BRG1-Deficient Non-Small Cell Lung Carcinomas. Research Square 2022. doi: 10.21203/rs.3.rs-1509537/v1.
27. Žitnik H, Chassagnon G, Canniff E, et al. SMARCA4/BRG1–Deficient Non–Small Cell Lung Carcinomas: Imaging features at baseline according to TTF-1 status. ECR 2023.
28. Nambirajan A, Singh V, Bhardwaj N, et al. SMARCA4/BRG1-Deficient Non-Small Cell Lung Carcinomas: A Case Series and Review of the Literature. Arch Pathol Lab Med 2021;145:90-8.
29. Crombé A, Alberti N, Villard N, et al. Imaging features of SMARCA4-deficient thoracic sarcomas: a multi-centric study of 21 patients. Eur Radiol 2019;29:4730-41.
30. Armon S, Hofman P, Ilié M. Perspectives and Issues in the Assessment of SMARCA4 Deficiency in the Management of Lung Cancer Patients. Cells 2021;10:1920.
31. Strobeck MW, DeCristofaro MF, Banine F, et al. The BRG-1 subunit of the SWI/SNF complex regulates CD44 expression. J Biol Chem 2001;276:9273-8.
32. Heidinger BH, Schwarz-Nemec U, Anderson KR, et al. Visceral Pleural Invasion in Pulmonary Adenocarcinoma: Differences in CT Patterns between Solid and Subsolid Cancers. Radiol Cardiothorac Imaging 2019;1:e190071.
33. Caso R, Connolly JG, Zhou J, et al. Preoperative clinical and tumor genomic features associated with pathologic lymph node metastasis in clinical stage I and II lung adenocarcinoma. NPJ Precis Oncol 2021;5:70.
34. Herpel E, Rieker RJ, Dienemann H, et al. SMARCA4 and SMARCA2 deficiency in non-small cell lung cancer: immunohistochemical survey of 316 consecutive specimens. Ann Diagn Pathol 2017;26:47-51.
35. Lin Y, Yu B, Sun H, et al. Promising efficacy of immune checkpoint inhibitor plus chemotherapy for thoracic SMARCA4-deficient undifferentiated tumor. J Cancer Res Clin Oncol 2023;149:8663-71.
36. Gantzer J, Davidson G, Vokshi B, et al. Immune-Desert Tumor Microenvironment in Thoracic SMARCA4-Deficient Undifferentiated Tumors with Limited Efficacy of Immune Checkpoint Inhibitors. Oncologist 2022;27:501-11.

Cite this article as: Kim JH, Woo JH, Lim CY, An T, Han J, Chung MJ, Cha YK. SMARCA4-deficient non-small cell lung carcinoma: clinicodemographic, computed tomography, and positron emission tomography-computed tomography features. J Thorac Dis 2024;16(3):1753-1764. doi: 10.21037/jtd-23-1606